Journal of Science and Transport Technology
Journal homepage: https://jstt.vn/index.php/en

Nonlinear dynamical response of FG sandwich plates with pores and flexibly constrained boundaries in thermal environments

Nguyen Van Thinh[1], Be Ngoc Son[2], Hoang Van Tung[3,*]
[1]Graduate University of Science and Technology, Vietnam Academy of Science and Technology, No. 18, Hoang Quoc Viet, Cau Giay, Hanoi, Vietnam
[2]RIMAS Research Group (Resilience & Innovative Materials for Smart Infrastructures), University of Transport Technology, 54 Trieu Khuc, Thanh Liet, Hanoi, Vietnam
[3]Faculty of Civil Engineering, Hanoi Architectural University, No. 129, Tran Phu, Ha Dong, Hanoi, Vietnam

Article info
Type of article:
Original research paper

DOI:
https://doi.org/10.58845/jstt.utt.2026.en.6.2.1-18

***Corresponding author:**
Email address:
tunghv@hau.edu.vn
hoangtung0105@gmail.com

Received: 14/10/2025
Received in Revised Form: 29/11/2025
Accepted: 17/12/2025

Abstract: The present article scrutinizes the nonlinear transient response (NTR) of functionally graded material (FGM) sandwich plates including the simultaneous impacts of pores, geometric perturbation, high temperature, and flexible constraints of boundaries. The characteristics of constitutive materials are depended on temperature and overall features of imperfect FGM are sought employing a modification of linear rule of mix. Two sandwich configurations fabricated from FGM and homogeneous layers are considered, and pores are evenly distributed in materials. Fundamental derivations via transverse displacement along with stress function (SF) are based on the first order plate theory (FOPT) incorporating initial geometric imperfection and von Kármán terms. The derived equations are resolved by adopting analytic solutions combined with Galerkin approach to yield a differential equation with nonlinear terms. The derived differential equation is resolved by virtue of taking up the Runge–Kutta integration diagram to graph the temporal transverse displacement (TD)–time curves of transient response of sandwich plates. An illustrative analysis is implemented to evaluate diverse impacts of pore volume ratio, imperfection, tangential restraints of boundaries, and high temperature on the nonlinear transient response. It is explored that in-plane edge confinements substantially influence the nonlinear dynamic response, especially at high temperatures. Furthermore, the thickness of skins and size of geometrical imperfection significantly affect temporal TD–time paths.
Keywords: FGM sandwich, Nonlinear transient response, Porosity, Elastic edge constraint, Temperature effects.

1. Introduction

Due to superior characteristics like high stiffness, remarkable ductility, prominent capacity of temperature withstanding, and preeminent integrity, FGM is broadly utilized in structural applications, especially in temperature shielding members. The statical and dynamical behavior of FG structures are attractive problems of evident

need. Praveen and Reddy [1] taken up finite element method (FEM) basing on the FOPT to investigate the NTR of FG flat panels with different boundary conditions in heated environments. Reddy [2] used analytical solutions and FEM on the basis of his third order plate theory (TOPT) to deal with the large-displacement static and transient response analyses of FG panels. Basing on the classical plate theory (CPT), the linear oscillation and transient behaviour of thin FG flat panels with initial compressive loads have been studied by Yang and Shen [3] utilizing one-dimensional differential quadrature (DQ) technique. Then this study was extended by Yang and Shen [4] for the linear transient investigation of thick FG flat panels employing the TODT. Using asymptotic solutions and TOPT, Huang and Shen [5, 6] perused the nonlinear oscillation and transient behaviour of FG plates without and with piezoelectric layers. By applying the FOPT and TOPT, Akbarzadeh et al. [7] conducted an analytical study on the small-deflection transient behavior of FG plates using Fourier series solutions. Using Navier series solutions along with numerous plate theories, Zenkour and Sobhy [8] explored the linear transient analysis of FG panels reposing on Pasternak foundations undergoing harmonic thermal loading. Ta and Noh [9] used the Navier series resolution on the basis of a refined theory of plate to analyze the linear transient response of FG plates with simply supported edges reposing elastic foundations. The nonlinear transient response of FG plates was treated by Bourihane et al. [10] taking up TOPT–based FEM in combination with an implicit algorithm. Kiani and coworkers [11, 12] executed the small-deflection static and transient analyses of FG panels with double curvature on elastic foundations taking advantage of analytical solutions and FOPT.

Large-displacement free and forced vibrational behaviour of FG structures is a subject of considerable importance. Sundararajan et al. [13] utilized the FOPT–based FEM to seek the frequencies of large-displacement free oscillation of FG plates exposed to thermal environments. Talha and Singh [14] executed a numerical investigation on the large–displacement free oscillation of higher order shear deformable FG flat panels taking full nonlinearity into consideration. The impacts of preexistent stresses and Pasternak–type foundations on the natural and nonlinear frequencies of free oscillations of FG panel components were examined by Shen and Wang [15] taking up asymptotic solution and TOPT. Gupta and Talha [16] presented a four–unknown TOPT and a numerical approach to peruse the influences of preexistent perturbations of plate geometry on the large-displacement free oscillation of FG panels. The nonlinear static and free oscillation analyses of FG flat panels were scrutinized by Cho [17] utilizing a method of 2D natural element. The nonlinear oscillation of FG plates with simple support and movable conditions at edges was performed by Alijani et al. [18] using the FOPT. The large–displacement oscillation analyses of thick FG plates and panels with double curvature have been executed in numerical investigations of Kar and Panda [19] and Lore et al. [20] employing a quasi-3D TOPT.

Due to outstanding characteristics such as effective sound and thermal insulations, excellent mechanical strength, and large ratio of rigidity to mass, the sandwich structures are extensively used in diverse fields and industries. Zenkour and coauthor [21, 22] taken up the sinusoidal-type plate theory and analytical solutions to explore the linear instability and free vibration responses of FG sandwich plates. The linear instability and free oscillation problems of FG sandwich plates were dealt with by Neves et al. [23, 24] taking advantage of quasi–3D TOPT along with mesh-free technique. Meiche et al. [25] taken up the Navier-type series solution basing on a four–unknown plate theory to investigate the linear instability and oscillation of FG sandwich plates. The linear bending and free vibration of FG sandwich plates were looked at in analytical investigation of Bessaim et al. [26] making use of a TOPT in which vertical shear

strains are hyperbolically distributed. The post-buckling behaviour of sandwich plates with FG skin sheets under mechanical loads was treated by Shen and Li [27] taking up a two-step asymptotic technique. Wang and Shen [28, 29] looked at the vibration, bending, thermal postbuckling and transient behaviours of high order shear deformable FG sandwich panels taking into consideration the impacts of elevated temperatures and foundation interactions. Basing on FOPT, Tung [30, 31] presented analytical investigations on the post-buckling behaviour of FGM sandwich plates and double curvature shells under thermal and thermomechanical loadings including geometric imperfection and displacement confinement of edges. Basing on an analytical derivation and TOPT, Dong et al. [32] explored the nonlinear instability of FG sandwich plates with oblique stiffeners undergoing compressive loads in thermal environments. The nonlinear instability of FG sandwich cylindrical shells integrated with spiral stiffeners has been perused by Nam et al. [33] using thin shell theory and Galerkin method.

During the fabricating process, pores can arise in the FGM and induce porosity of this material. Accordingly, the impacts of pores on the static and dynamical behaviours of FG components should be addressed. The small- and large-amplitude oscillations of thin and moderate thick FG beams with pores and flexibly confined ends were explored in articles [34, 35]. The impacts of pores on the small-amplitude free oscillation of porous FG rectangular plates was perused in works [36-38] taking up various plate theories and methods. Zghal and Dammak [39] employed the improved FOPT–based FEM to seek the frequencies of linear free oscillation of FG flat panels and spherical shells with porosity. The linear oscillation of porous FG double curvature shell panels was treated in studies of Trang et al. [40] adopting an analytical approach and Abuteir and Boutagouga [41] employing FEM. Basing on various plate theories, the large–amplitude free oscillation of porous FG flat panels was examined by Xie et al. [42] utilizing energy balance method. The TOPT–based FEM was employed in works of Ramteke and coauthors [43, 44] perusing the nonlinear oscillation of FG double curvature panels with porosity and various boundary conditions. The influences of pores and preexistent stresses on the large-amplitude free vibration of thin FG plates are addressed by Anh et al. [45] taking advantage of CPT. Within the framework of the FOPT, the impacts of pore and flexible boundary constraint on the large-displacement free oscillation and instability of FG circular plates, spherical caps and doubly curved shell panels have been scrutinized in papers [46-49]. Recently, the linear free vibration and bending behaviours of FG sandwich double curvature panels with porosity have been examined by Lakhdar et al. [50] taking up of TOPT and FEM. It is evident from the open literature that the large-displacement transient response of FG sandwich plate components with pores and elastically confined boundaries have been not investigated.

To full the aforementioned lack, in the present study, the nonlinear transient response of FG sandwich plates with pores undergone high temperatures and sudden uniform transverse pressure is analyzed. Two types of sandwich configurations possessing FGM core and face sheets are considered. The pores are taken into FGM according to even type. The properties of constitutive materials are depended on temperature and effective properties of imperfect FGM are evaluated due to applying a modification of linear mixture rule. All edges of plate are simply supported and flexibly confined against tangential displacements. Equations regarding motion and compatibility conditions are formulated on the basis of the FOPT accompanying von Kármán nonlinearities and initial geometric imperfection of plate shape. These equations are solved by means of analytical solutions in combination with Galerkin method to derive a time differential equation including nonlinear terms. This differential equation is solved by taking advantage of Runge–Kutta

scheme to trace temporal displacement–time paths of nonlinear transient response of porous FG sandwich plates. Illustrative examinations are executed to rate numerous impacts on nonlinear transient response, and insightful discussions are given.

2. FG sandwich plates and material properties

This work studies a structural model in form of a rectangular sandwich plate (i.e. flat panel) of longitudinal dimension a, width b and total thickness h. The sandwich panel is constructed from homogeneous and FGM layers. The panel is reposed in a Cartesian axes system with, x, y, z axes represent the length, width, thickness directions, respectively, such that definite regions are $x \in [0,a]$, $y \in [0,b]$ and $z \in [-h/2, h/2]$, as exhibited in Fig. 1. The sandwich panel is manufactured from two thinner face sheets (i.e. skin layers) combined with a thicker core layer. The thickness of each face sheet is h_f and the core layer is perfectly bonded with face sheets. This work examines two sandwich plate configurations with FGM and homogeneous face layers and are respectively mentioned to as sandwich panels of types A and B [30, 31].

2.1. Type A of sandwich panel: homogeneous core and FGM skin layers

In this sandwich configuration, the plate is fabricated from metal homogeneous core layer and FGM face sheets, as depicted in Fig. 2a. The upper and lower surfaces of the plate are ceramic–rich and the volume ratio of ceramic is gradually reduced from surfaces to interfaces. This model of FG sandwich panel of type A is symmetric about middle plane and the volume percentage of metal portion is defined by virtue of a power law distribution as the below [30, 31]

$$V_m = \left(\frac{z-h_0}{h_1-h_0}\right)^N,\ h_0 \le z \le h_1,\ \text{top skin}$$
$$V_m = 1,\ h_1 \le z \le h_2,\ \text{core layer} \quad (1)$$
$$V_m = \left(\frac{z-h_3}{h_2-h_3}\right)^N,\ h_2 \le z \le h_3,\ \text{bottom skin}$$

where N is a nonnegative value known as index of volume fraction. In the above $h_0 = -h/2$, $h_1 = -h/2 + h_f$, $h_2 = h/2 - h_f$, and $h_3 = h/2$.

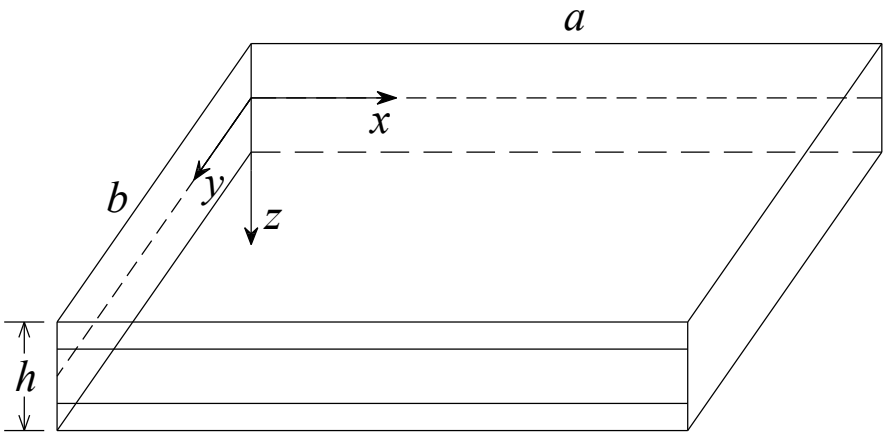

Fig. 1. Geometry and axis system of a sandwich flat panel

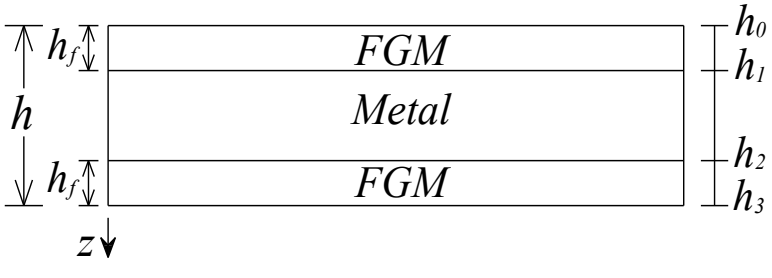

(a)

Fig. 2. The considered sandwich panel configurations

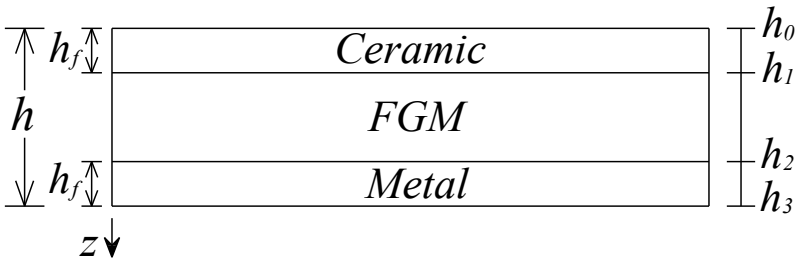

(b)

Fig. 2. (continued)

2.2. Type B of sandwich panel: FGM core and homogeneous face layers

For this type of sandwich model, the plate is constructed from homogeneous face sheets and a FGM core layer, as depicted in Fig. 2b. Specifically, the upper and bottom face sheets are respectively fabricated of homogeneous ceramic and metal, meanwhile the ceramic percentage in the FGM core is smoothly dropped from upper interface to lower interface. This arrangement makes the type B of sandwich panel asymmetrical about middle surface and the percentage of metal material is evaluated as follows [30, 31]

$$V_m = 0,\ h_0 \le z \le h_1,\ \text{top skin}$$

$$V_m = \left(\frac{z-h_1}{h_2-h_1}\right)^N,\ h_1 \le z \le h_2,\ \text{core layer} \qquad (2)$$

$$V_m = 1,\ h_2 \le z \le h_3,\ \text{bottom skin}$$

In the considered configurations of sandwich components, the volume ratio of ceramic material is calculated by means of $V_c = 1 - V_m$.

Pores probably exist in the fabricating progress and render FGM imperfect. Because of the presence of pores, the effective properties P_{eff} of imperfect FGM can be determined by means of a modified rule of mixture as follows [34]

$$P_{eff} = P_c\left(V_c - \frac{\xi}{2}\right) + P_m\left(V_m - \frac{\xi}{2}\right) \qquad (3)$$

where P implies a particular property like Young's modulus E, thermal expansion coefficient (TEC) α, and the density ρ. Additionally, ξ is a small value ($0 \le \xi \ll 1$) known as the percentage of volume of pores. When ξ is zero–valued, material is absent from porosity, i.e. perfect material. In the presented study, the pores are hypothesized to spread into three layers of sandwich plate obeying an even type and the effective properties of imperfect FGM are computed as [34]

$$P_{eff} = (P_m - P_c)V_m + P_c - \frac{\xi}{2}(P_m + P_c) \qquad (4)$$

In as much as the dependence of Poisson's ratio on position, temperature and porosity is very weak, the effective Poisson's coefficient ν of porous FGM is taken as a constant in the present study.

3. Basic derivations

In the considered study, the sandwich plate is assumed to be moderately thick and geometrically imperfect. It is well–known that the FOPT is of less computation cost and good accuracy for plates with moderate thickness. In this study, the FOPT is taken up to establish the motion and compatibility equations. Based on the FOPT, the strain components at a distance z from the middle surface incorporating the effects of von Kármán nonlinearities and initial geometric imperfection are expressed as [51]

$$\begin{pmatrix}\varepsilon_x\\ \varepsilon_y\\ \gamma_{xy}\end{pmatrix} = \begin{pmatrix}\varepsilon_x^0\\ \varepsilon_y^0\\ \gamma_{xy}^0\end{pmatrix} + z\begin{pmatrix}\varepsilon_x^1\\ \varepsilon_y^1\\ \gamma_{xy}^1\end{pmatrix},\ \begin{pmatrix}\gamma_{xz}\\ \gamma_{yz}\end{pmatrix} = \begin{pmatrix}\phi_x + w_{,x}\\ \phi_y + w_{,y}\end{pmatrix} \qquad (5)$$

in which

$$\begin{pmatrix}\varepsilon_x^0\\ \varepsilon_y^0\\ \gamma_{xy}^0\end{pmatrix} = \begin{pmatrix} u_{,x} + w_{,x}^2/2 + w_{,x}w_{,x}^*\\ v_{,y} + w_{,y}^2/2 + w_{,y}w_{,y}^*\\ u_{,y} + v_{,x} + w_{,x}w_{,y} + w_{,x}w_{,y}^* + w_{,y}w_{,x}^*\end{pmatrix},$$

$$\begin{pmatrix}\varepsilon_x^1\\ \varepsilon_y^1\\ \gamma_{xy}^1\end{pmatrix} = \begin{pmatrix}\phi_{x,x}\\ \phi_{y,y}\\ \phi_{x,y} + \phi_{y,x}\end{pmatrix} \qquad (6)$$

where u, v are membrane components of displacements in the x, y axes, respectively, and w is transverse displacement (i.e. deflection) of a corresponding point on the middle plane. In the above, ϕ_x and ϕ_y are the rotations of a transverse normal about the y and x axes, respectively, and w^* is a definite function manifesting initial geometric imperfection.

Stress components are determined by means of constitutive relations combining with temperature effects as

$$\sigma_x = \frac{E}{1-\nu^2}\left[\varepsilon_x + \nu\varepsilon_y - (1+\nu)\alpha\Delta T\right]$$
$$\sigma_y = \frac{E}{1-\nu^2}\left[\varepsilon_y + \nu\varepsilon_x - (1+\nu)\alpha\Delta T\right] \quad (7)$$
$$(\sigma_{xy}, \sigma_{xz}, \sigma_{yz}) = \frac{E}{2(1+\nu)}(\gamma_{xy}, \gamma_{xz}, \gamma_{yz})$$

where $\Delta T = T - T_0$ is uniform temperature rise from an ambient value T_0 to a higher temperature. The internal force and moment intensities are determined through stresses as

$$(N_x, N_y, N_{xy}) = \int_{-h/2}^{h/2} (\sigma_x, \sigma_y, \sigma_{xy}) dz,$$
$$(Q_x, Q_y) = K_S \int_{-h/2}^{h/2} (\sigma_{xz}, \sigma_{yz}) dz \quad (8)$$
$$(M_x, M_y, M_{xy}) = \int_{-h/2}^{h/2} (\sigma_x, \sigma_y, \sigma_{xy}) z dz$$

here K_S is coefficient of shear correctness taken a value as 5/6 in the numerical results. By placing Eqs. (7) into Eqs. (8), the above intensities have the form

Eqs. (9)

with Eqs. (10)

Membrane and rotatory inertias are hypothesized to be small and omitted in the present work. Obeying these assumptions and the FOPT, the equation of motion of a porous FG sandwich flat panel takes the form [30, 49]

Eqs. (11)

with t is time, q is uniform transverse pressure suddenly applied on the top surface of plate, and f is a SF concerned as $N_x = f_{,yy}, N_y = f_{,xx}, N_{xy} = -f_{,xy}$. Additionally, in the above, I_0, D and ∇^2 symbolize the mass moment of inertia, bending rigidity, and planar Laplace's operator, respectively, the expressions of which are the following

Eqs. (12)

Relation for strain compatibility of porous FG sandwich panel can be exhibited as the below form [30]

Eqs. (13)

In the presented analysis, all edges of sandwich panel are simply supported and flexibly constrained against membrane displacements. The described edge conditions are manifested in the form

Eqs. (14a) (14b)

with N_{x0} and N_{y0} are resultants of reactive forces generated at the confined sides $x = 0, a$ and $y = 0, b$, respectively. These resultants have concernment with average end–shriveling quantities at corresponding edge pairs as [30]

Eqs. (15)

in which c_1 and c_2 are tangential stiffness parameters of elastic springs representing membrane confinements of opposite boundaries $x = 0, a$ and $y = 0, b$, respectively. It is easily observed that freely movable, immovable and partially movable edges $x = 0, a$ are corresponded with $c_1 = 0$, $c_1 \to \infty$ and $0 < c_1 < \infty$. Similarly, the values of $c_2 = 0$, $c_2 \to \infty$ and $0 < c_2 < \infty$ respectively manifest freely movable, immovable and partially movable conditions of edges $y = 0, b$.

In the view of relations (6) and (9), the results of $\partial u / \partial x$ and $\partial v / \partial y$ can be determined, and Eqs. (15) can be manifested in the form

Eqs. (16a) (16b)

4. Analytical solution procedure

In order to fulfill the boundary conditions (15), the below analytical solutions are employed [52]

Eqs. (17a) (17b) (17c)

where $\beta_m = m\pi/a$, $\delta_n = n\pi/b$ and m,n are positive integers representing vibration mode. In addition, W is maximum value of transverse displacement and μ is a small value representing size of imperfection in the shape. By substituting the solutions (17a, b) into the equation of strain compatibility (13), the time-dependent coefficients $A_i\,(i=1,2,3)$ in the SF are sought as follows

Eqs. (18)

By using relations (6) and (9) into two among five motion equations and introducing the expressions (17a, c) into the resulting relations, we can determine the time-dependent coefficients of rotations as follows [30]

Eqs. (19)

in which

Eqs. (20)

Putting solutions (17a, b) into the motion equation (11) and taking up Galerkin procedure to the resulting relation yields

Eqs. (21)

where

Eqs. (22)

in which

Eqs. (23)

Substitution of the solutions (17) into relations (16) results in the below expressions of reactive force resultants

Eqs. (24a) (24b)

where coefficients e_{ij} $(i=1,2; j=1,2,3)$ are similar to coefficients provided in the paper [30] and omitted here for the purpose of briefness. By placing Eqs. (24) into the Eq. (21) leads to the below equation

Eqs. (25)

where

Eqs. (26)

Eq. (25) is a nonlinear differential equation representing the nonlinear transient response of FG sandwich plates with pores and all flexibly restrained edges in the thermal environments. The deflection – time paths are traced by means of Runge–Kutta integration scheme with conditions at initial time are $W(0)=0$ and $\dot{W}(0)=0$.

$$\left(N_x,M_x\right)=\frac{1}{1-\nu^2}\left[\left(E_1,E_2\right)\left(\varepsilon_x^0+\nu\varepsilon_y^0\right)+\left(E_2,E_3\right)\left(\varepsilon_x^1+\nu\varepsilon_y^1\right)\right]-\frac{1}{1-\nu}\left(\Phi_0,\Phi_1\right)$$

$$\left(N_y,M_y\right)=\frac{1}{1-\nu^2}\left[\left(E_1,E_2\right)\left(\varepsilon_y^0+\nu\varepsilon_x^0\right)+\left(E_2,E_3\right)\left(\varepsilon_y^1+\nu\varepsilon_x^1\right)\right]-\frac{1}{1-\nu}\left(\Phi_0,\Phi_1\right)$$

$$\left(N_{xy},M_{xy}\right)=\frac{1}{2\left(1+\nu\right)}\left[\left(E_1,E_2\right)\gamma_{xy}^0+\left(E_2,E_3\right)\gamma_{xy}^1\right]$$

$$\left(Q_x,Q_y\right)=\frac{E_1}{2\left(1+\nu\right)}K_S\left(\phi_x+w_{,x},\phi_y+w_{,y}\right) \qquad (9)$$

$$\left(E_1,E_2,E_3\right)=\int_{-h/2}^{h/2}E\left(1,z,z^2\right)dz\,,\ \left(\Phi_0,\Phi_1\right)=\int_{-h/2}^{h/2}E\alpha\Delta T\left(1,z\right)dz \qquad (10)$$

$$D\nabla^4 w+\frac{2\left(1+\nu\right)}{K_S E_1}D\nabla^2\left[f_{,yy}\left(w_{,xx}+w^*_{,xx}\right)-2f_{,xy}\left(w_{,xy}+w^*_{,xy}\right)+f_{,xx}\left(w_{,yy}+w^*_{,yy}\right)-I_0 w_{,tt}\right]$$

$$-f_{,yy}\left(w_{,xx}+w^*_{,xx}\right)+2f_{,xy}\left(w_{,xy}+w^*_{,xy}\right)-f_{,xx}\left(w_{,yy}+w^*_{,yy}\right)-q+I_0 w_{,tt}=0 \qquad (11)$$

$$I_0=\int_{-h/2}^{h/2}\rho dz\,,\ D=\frac{E_1E_3-E_2^2}{E_1\left(1-\nu^2\right)}\,,\ \nabla^2\equiv\frac{\partial^2}{\partial x^2}+\frac{\partial^2}{\partial y^2} \qquad (12)$$

$$\nabla^4 f-E_1\left(w_{,xy}^2-w_{,xx}w_{,yy}+2w_{,xy}w^*_{,xy}-w_{,xx}w^*_{,yy}-w_{,yy}w^*_{,xx}\right)=0 \qquad (13)$$

$$w=\phi_y=N_{xy}=M_x=0\,,\ N_x=N_{x0}\ \text{at}\ x=0,a \qquad (14a)$$

$$w = \phi_x = N_{xy} = M_y = 0,\ N_y = N_{y0} \text{ at } y = 0, b \qquad (14b)$$

$$N_{x0} = -\frac{c_1}{ab}\int_0^a\int_0^b \frac{\partial u}{\partial x}dydx\ ,\ N_{y0} = -\frac{c_2}{ab}\int_0^a\int_0^b \frac{\partial v}{\partial y}dydx \qquad (15)$$

$$N_{x0} = -\frac{c_1}{ab}\int_0^a\int_0^b \left[\frac{1}{E_1}\left(f_{,yy} - \nu f_{,xx}\right) - \frac{E_2}{E_1}\phi_{x,x} - \frac{1}{2}w_{,x}^2 - w_{,x}w_{,x}^* + \frac{\Phi_0}{E_1}\right]dydx \qquad (16a)$$

$$N_{y0} = -\frac{c_2}{ab}\int_0^a\int_0^b \left[\frac{1}{E_1}\left(f_{,xx} - \nu f_{,yy}\right) - \frac{E_2}{E_1}\phi_{y,y} - \frac{1}{2}w_{,y}^2 - w_{,y}w_{,y}^* + \frac{\Phi_0}{E_1}\right]dydx \qquad (16b)$$

$$w(x,y,t) = W(t)\sin\beta_m x \sin\delta_n y\ ,\ w^*(x,y) = \mu h \sin\beta_m x \sin\delta_n y \qquad (17a)$$

$$f(x,y,t) = A_1(t)\cos 2\beta_m x + A_2(t)\cos 2\delta_n y + A_3(t)\sin\beta_m x \sin\delta_n y + \frac{1}{2}N_{x0}y^2 + \frac{1}{2}N_{y0}x^2 \qquad (17b)$$

$$\phi_x(x,y,t) = B_1(t)\cos\beta_m x \sin\delta_n y\ ,\ \phi_y(x,y,t) = B_2(t)\sin\beta_m x \cos\delta_n y \qquad (17c)$$

$$A_1(t) = \frac{E_1\delta_n^2}{32\beta_m^2}W\left(W + 2\mu h\right)\ ,\ A_2(t) = \frac{E_1\beta_m^2}{32\delta_n^2}W\left(W + 2\mu h\right)\ ,\ A_3(t) = 0 \qquad (18)$$

$$B_1(t) = \frac{b_{13}b_{22} - b_{12}b_{23}}{b_{11}b_{22} - b_{12}^2}W\ ,\ B_2(t) = \frac{b_{23}b_{11} - b_{12}b_{13}}{b_{11}b_{22} - b_{12}^2}W \qquad (19)$$

$$b_{11} = D\beta_m^2 + \frac{1-\nu}{2}D\delta_n^2 + \frac{K_S E_1}{2(1+\nu)}\ ,\ b_{22} = D\delta_n^2 + \frac{1-\nu}{2}D\beta_m^2 + \frac{K_S E_1}{2(1+\nu)}\ ,$$

$$b_{12} = \frac{1+\nu}{2}D\beta_m\delta_n\ ,\ b_{13} = -\frac{K_S E_1\beta_m}{2(1+\nu)}\ ,\ b_{23} = -\frac{K_S E_1\delta_n}{2(1+\nu)} \qquad (20)$$

$$s_{11}\frac{d^2\overline{W}}{dt^2} + s_{21}\overline{W} + s_{31}\overline{W}\left(\overline{W} + \mu\right)\left(\overline{W} + 2\mu\right) + s_{41}\left(m^2B_a^2\bar{N}_{x0} + n^2\bar{N}_{y0}\right)\left(\overline{W} + \mu\right) = s_{51}B_h q \qquad (21)$$

$$B_a = \frac{b}{a}\ ,\ \left(\bar{N}_{x0}, \bar{N}_{y0}, \overline{W}\right) = \frac{1}{h}\left(N_{x0}, N_{y0}, W\right)\ ,\ s_{11} = \rho_1 h^2 S_{mn}\ ,\ s_{21} = \frac{\pi^4}{B_h^4}\bar{D}\left(m^2B_a^2 + n^2\right)^2$$

$$s_{31} = \frac{\bar{E}_1\pi^4}{16B_h^4}\left(m^4B_a^4 + n^4\right)S_{mn}\ ,\ s_{41} = \frac{\pi^2}{B_h^2}S_{mn}\ ,\ s_{51} = \frac{16\gamma_m\gamma_n}{mn\pi^2 B_h} \qquad (22)$$

$$\left(\bar{E}_1, \rho_1, B_h\right) = \frac{1}{h}\left(E_1, I_0, b\right)\ ,\ \bar{D} = \frac{D}{h^3}\ ,\ \gamma_k = \frac{1}{2}\left[1 - (-1)^k\right]\quad (k = m,n)\ ,$$

$$S_{mn} = \frac{2(1+\nu)\bar{D}\pi^2}{K_S\bar{E}_1 B_h^2}\left(m^2B_a^2 + n^2\right) + 1 \qquad (23)$$

$$\bar{N}_{x0} = e_{11}\overline{W} + e_{12}\overline{W}\left(\overline{W} + 2\mu\right) - e_{13}G\Delta T \qquad (24a)$$

$$\bar{N}_{y0} = e_{21}\overline{W} + e_{22}\overline{W}\left(\overline{W} + 2\mu\right) - e_{23}G\Delta T \qquad (24b)$$

$$s_{11}\frac{d^2\overline{W}}{dt^2} + s_{21}\overline{W} + s_{22}\overline{W}\left(\overline{W} + \mu\right) + s_{32}\overline{W}\left(\overline{W} + \mu\right)\left(\overline{W} + 2\mu\right) + s_{42}\left(\overline{W} + \mu\right)\Delta T = s_{51}B_h q \qquad (25)$$

$$s_{22} = s_{41}\left(e_{11}m^2B_a^2 + e_{21}n^2\right)\ ,\ s_{32} = s_{31} + s_{41}\left(e_{12}m^2B_a^2 + e_{22}n^2\right),$$

$$s_{42} = s_{41}\left(e_{13}m^2B_a^2 + e_{23}n^2\right)G\ ,\ G = \frac{1}{h}\int_{-h/2}^{h/2} E\alpha dz \qquad (26)$$

5. Numerical results and discussion

There is no previous analysis on the nonlinear transient response (NTR) of FG sandwich plates with pores. To validate the present work, nonlinear transient behaviour of a FG single-layered plate is carried out. The result for FG single-layered plate is easily obtained from the present formulation by letting of thickness of face sheet of the sandwich plate of type B zero-valued. Specifically, the NTR of a Al/ZrO_2 plate with immovable boundary edges and without porosity under uniform pressure loading $q = 10^6\,N/m^2$ is examined. The properties of these constituents are $E_m = 70\,GPa$, $\alpha_m = 23\times10^{-6}/^0\,C$, $\rho_m = 2707\,kg/m^3$, $\nu_m = 0.3$ for Al and $E_c = 151GPa$, $\alpha_c = 10.0\times10^{-6}/^oC$, $\rho_c = 3000\,kg/m^3$, $\nu_c = 0.3$ for ZrO_2 [1].

Non–dimensional deflection–time relation path is graphed by taking up Eq. (25) and compared in Fig. 3 along with analysis reported by Praveen and Reddy [1] applying FOPT along with FEM. Within the comparison, non–dimensional quantities of central transverse displacement W^* and time t^* are calculated as the below [1]

$$W^* = \frac{E_m h}{qa^2}W\ ,\quad t^* = t\sqrt{\frac{E_m}{a^2\rho_m}} \tag{27}$$

In addition, to correspond to indication in the article [1], the z axis is with upward positive side and the upper $(z = h/2)$ and bottom $(z = -h/2)$ planes of the Al/ZrO_2 plate are ceramic–rich and metal–rich, respectively, in the Fig. 3. Volume fraction index p corresponding to this case is defined as $V_c = (1/2 + z/h)^p$. As can be found, the present response path well agrees with that plotted in the paper [1].

In what follows, various effects on the NTR of porous sandwich plates fabricated from Si_3N_4 and SUS304 will be analyzed. The temperature–dependent (T-D) properties like Young's modulus E and TEC α of Si_3N_4 and SUS304 have been given in preceding studies, e.g. [4, 5], and are not displayed here for the purpose of briefness. The density values of constitutive materials are $\rho_c = 2370\,kg/m^3$ and $\rho_m = 8166\,kg/m^3$ for Si_3N_4 and SUS304, respectively. Poisson's coefficient of Si_3N_4/SUS304 FGM is taken to be $\nu = 0.28$ [4, 5]. The geometries of the plate are $h = 0.02\,m$, $a/b = 1$, $b/h = 20$. The defection mode shape and uniform pressure are respectively assumed to be $(m,n) = (1,1)$ and $q = 10\times10^6\,N/m^2$. Furthermore, the porous FG sandwich plates are assumed to be of perfect geometry ($\mu = 0$) and located at ambient temperature, unless otherwise mentioned. In numerical results, the effect of in-plane constraints of edges will be measured by dimensionless quantities as [30]

$$\lambda_1 = \frac{c_1}{E_1^0 + c_1}\ ,\ \lambda_2 = \frac{c_2}{E_1^0 + c_2} \tag{28}$$

in which E_1^0 is result of E_1 valued at room temperature $T_0 = 300\,K$. The above formulae indicate that the values of $\lambda_1 = 0$, $\lambda_1 = 1$ and $0 < \lambda_1 < \infty$ represents freely movable, immovable and partially movable edges $x = 0, a$, respectively. Also, the values of $\lambda_2 = 0$, $\lambda_2 = 1$ and $0 < \lambda_2 < \infty$ exhibit freely movable, fully immovable and partially movable cases of edges $y = 0, b$, respectively.

Illustrative analyses are graphically presented in the form of double figures with a and b parts corresponding to sandwich plates of types A and B, respectively. First, the influences of porosity volume ratio ξ on the NTR of sandwich plates with immovable edges ($N = 0.2$, $h_f/h = 0.1$) are shown in Fig. 4. As can be found, the dynamical transverse displacement is obviously increased when the percentage of pores is increased. Quantitatively, in Fig. 4a, the amplitude of transverse displacement is raised about 10 percent when the ξ is increased from 0 to 0.1. It is attributed to decrease in the flexural rigidity of the

plate when the ξ is increased. Although the bending withstanding ability of the sandwich panel is evidently weakened because of increase in the ξ, the oscillation period of the panel is slightly affected due to variation of pore percentage. Next, the impacts of volume fraction index N on the nonlinear temporal behaviour of porous sandwich plates with immovable edges ($\xi = 0.1,\ h_f / h = 0.1$) are graphed in Fig. 5. As can be realized, the dynamical deflection (DD) and period of vibration (PoV) are substantially reduced by virtue of the increase in the N index. Furthermore, it seems that the impacts of the N value on the large-displacement dynamical response of sandwich plates of type B are more considerable.

The impacts of h_f / h ratio on the large-deflection temporal behaviour of sandwich plates with porosity and immovable edges are examined in Fig. 6. It is revealed that for the sandwich plates of type A, the amplitude of DD and PoV are fundamentally decreased as a result of enhancement of the h_f / h ratio. It is attributed to the increasing in the bending stiffness of FGM/SUS304/FGM sandwich plates as the thickness of FGM face sheets are augmented. Meanwhile, the h_f / h ratio marginally affects the NTR of sandwich plates of type B. The dynamical displacement of Si_3N_4/FGM/SUS304 plates are very slightly raised as the h_f / h ratio is larger.

Next, the effects of in-plane constraints of boundary edges on the NTR of porous sandwich plates ($\xi = 0.1, h_f / h = 0.1$) are positioned at ambient and elevated temperatures are plotted in Figs. 7 and 8, respectively. It is found from Fig. 7 that the DD and PoV of the panel placed at ambient temperature ($T = 300\,K$) are decreased when the edges are restrained more severely, i.e. λ_1, λ_2 parameters are larger. Conversely, when the plate is placed to an higher temperature ($T = 500\,K$), Fig. 8 indicates that the amplitude of DD and PoV are enhanced due to more rigorous restraint of edges. It is attributable to thermally caused forces at constrained edges rendering the DD of the panel larger. Concretely, the thermal forces at constrained edges are larger when the constraints of boundary edges are more severe and temperature is higher.

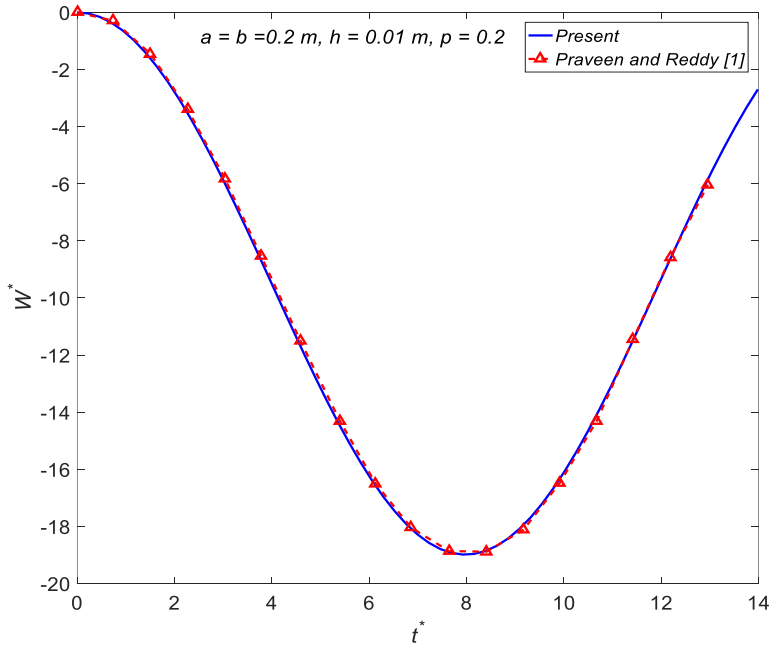

Fig. 3. Large-displacement transient paths of simply supported Al / ZrO_2 plates with immovable boundary edges under sudden uniform load of $q = 1.0 \times 10^6\ N/m^2$ ($\Delta T = 0$)

The influences of thermal environments on the NTR of porous sandwich plates with partially movable edges ($\xi = 0.1, h_f / h = 0.1, \lambda_1 = \lambda_2 = 0.5$) are depicted in Fig. 9. It is obvious that the amplitude of DD and PoV of sandwich plates are prominently increased in case the temperature is more elevated.

Finally, the influences of initial geometric imperfection on the NTR of porous sandwich plates with immovable edges at room and high values of temperature are exhibited in Figs. 10 and 11, respectively. As can be seen, geometric imperfection has significant influence on the temporal behavior of sandwich plates. Specifically, it is interesting to note that the period of forced vibration and the amplitude of dynamical transverse displacement are remarkably dropped in case the size of geometric perturbation is increased.

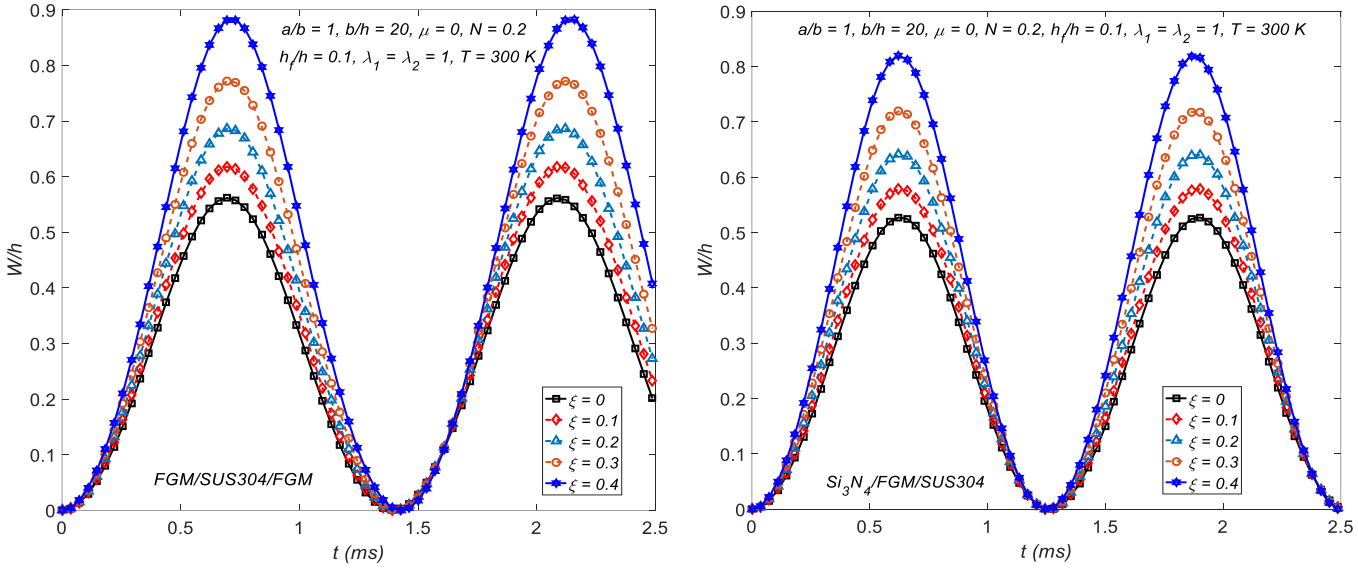

(a) (b)

Fig. 4. Impacts of pore volume percentage on NTR of sandwich plates with immovable edges: FGM/SUS304/FGM and (b) Si_3N_4/FGM/ SUS304

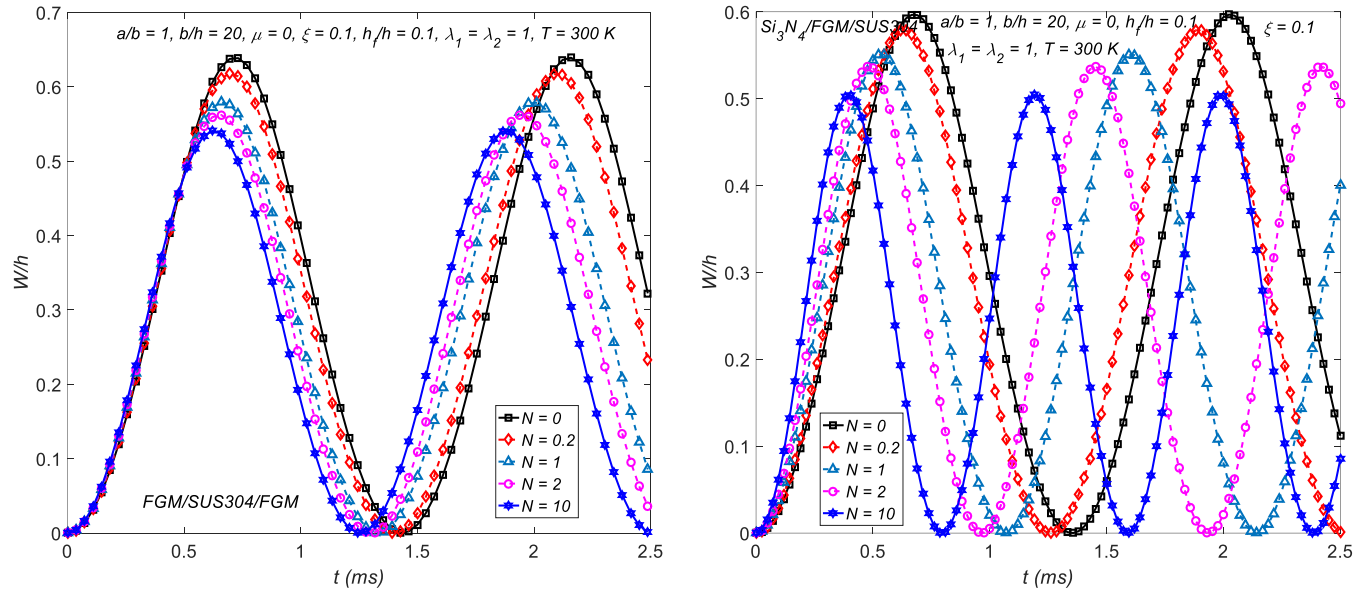

(a) (b)

Fig. 5. Impacts of volume fraction index on NTR of sandwich plates with immovable edges: (a) FGM/SUS304/FGM and (b) Si_3N_4/FGM/ SUS304

6. Concluding remarks

A semi-analytical investigation on NTR of FG sandwich plates with pores and flexibly constrained edges in the thermal environments has been executed. Basing on the above discussions, the closure remarks are provided as the below:

(i) The pores detrimentally affect the dynamical bending response of FG sandwich plates and the amplitude of DD is prominently augmented when the volume ratio of pores is raised.

(ii) The amplitudes of dynamic deflections of sandwich plates exposed to room and higher temperatures are lowered and raised, respectively, as the boundary edges are constrained more severely.

(iii) Elevated temperature substantially influences the NTR of FG sandwich plate components. The enhancement of temperature makes the amplitude of dynamical deflection and the period of vibration larger.

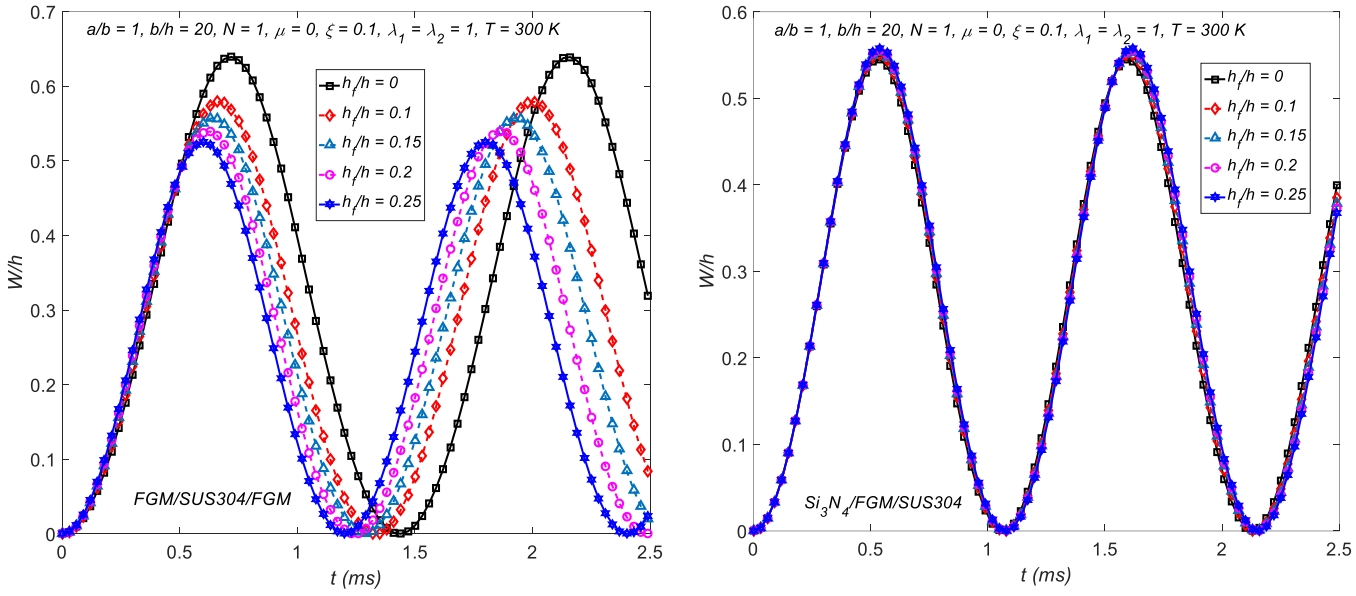

Fig. 6. Impacts of thickness of face sheets on the NTR of sandwich plates with immovable edges: (a) FGM/SUS304/FGM and (b) Si_3N_4/FGM/ SUS304

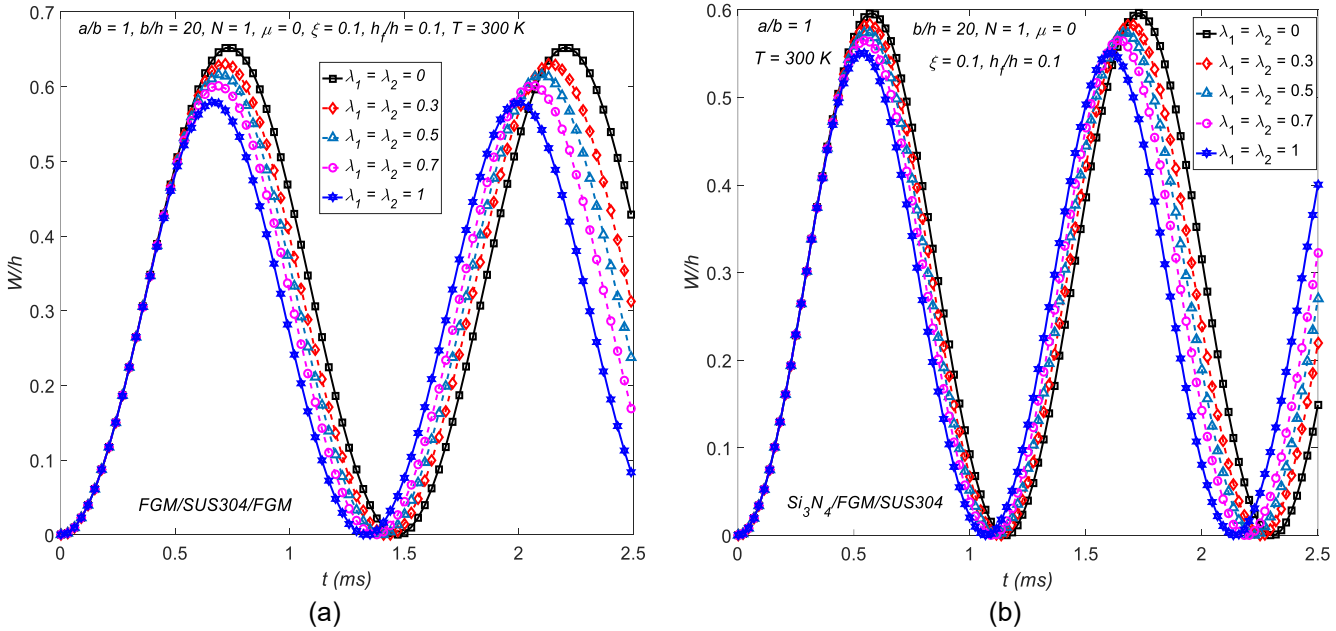

Fig. 7. Effects of tangential edge constraints on NTR of sandwich panels at room temperature: (a) FGM/SUS304/FGM and (b) Si_3N_4/FGM/ SUS304

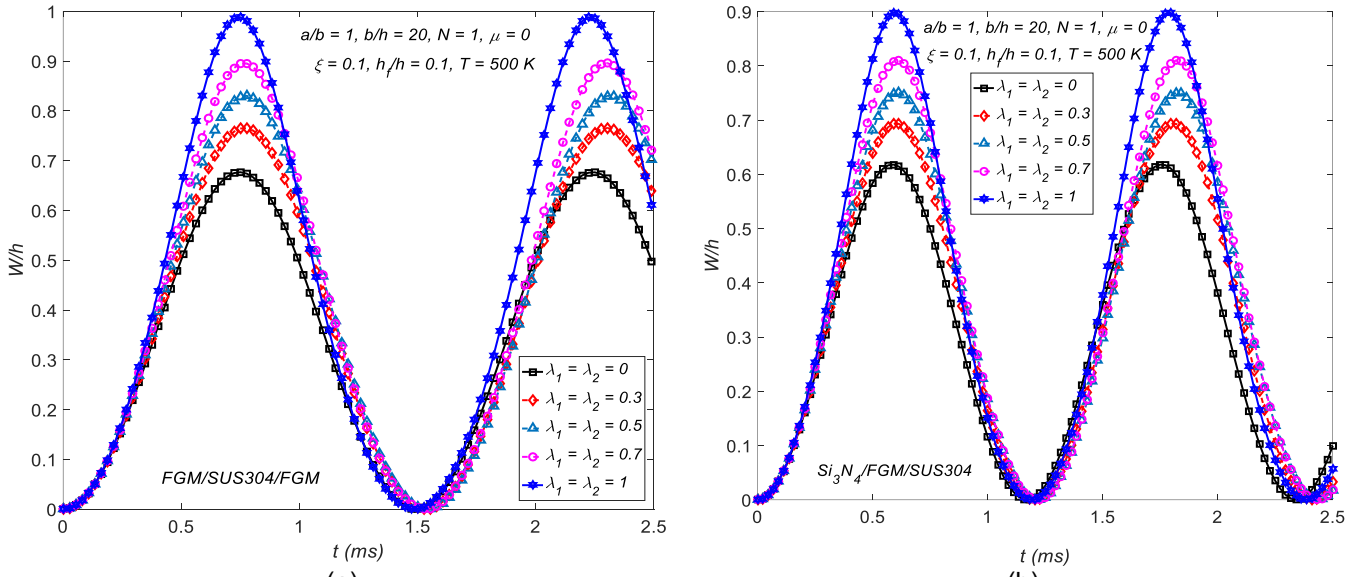

(a) (b)

Fig. 8. Effects of tangential edge constraints on NTR of sandwich panels at a higher temperature; FGM/SUS304/FGM and (b) Si_3N_4/FGM/ SUS304

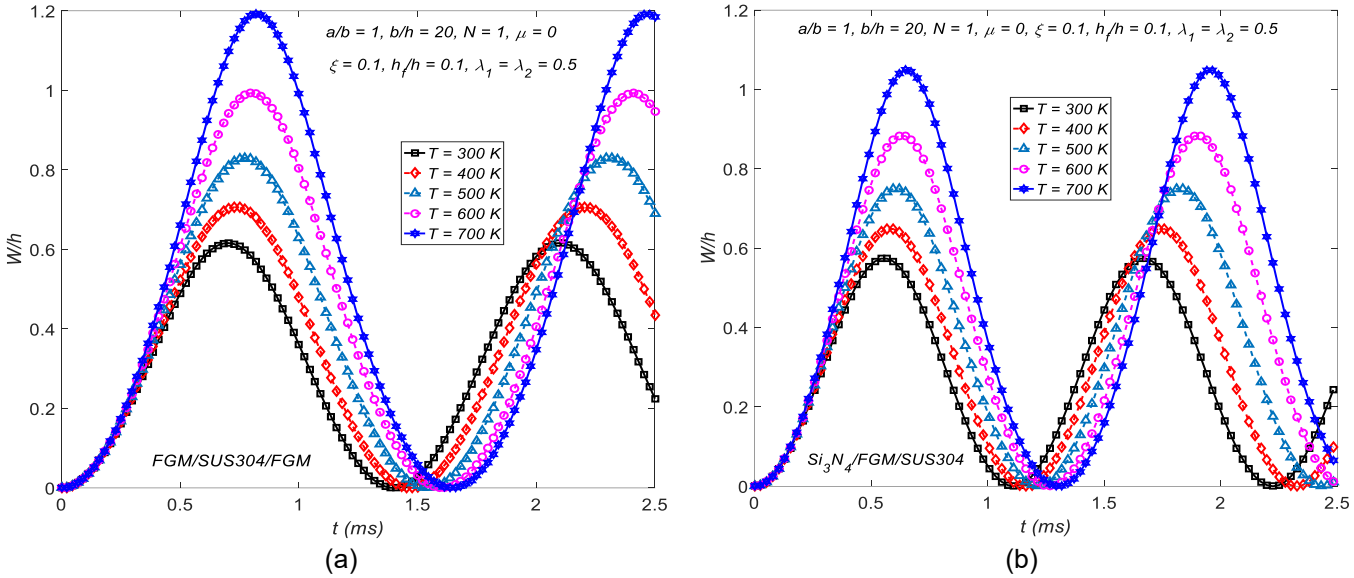

(a) (b)

Fig. 9. Effects of thermal environments on the NTR of sandwich panels with partially movable edges; FGM/SUS304/FGM and (b) Si_3N_4/FGM/ SUS304

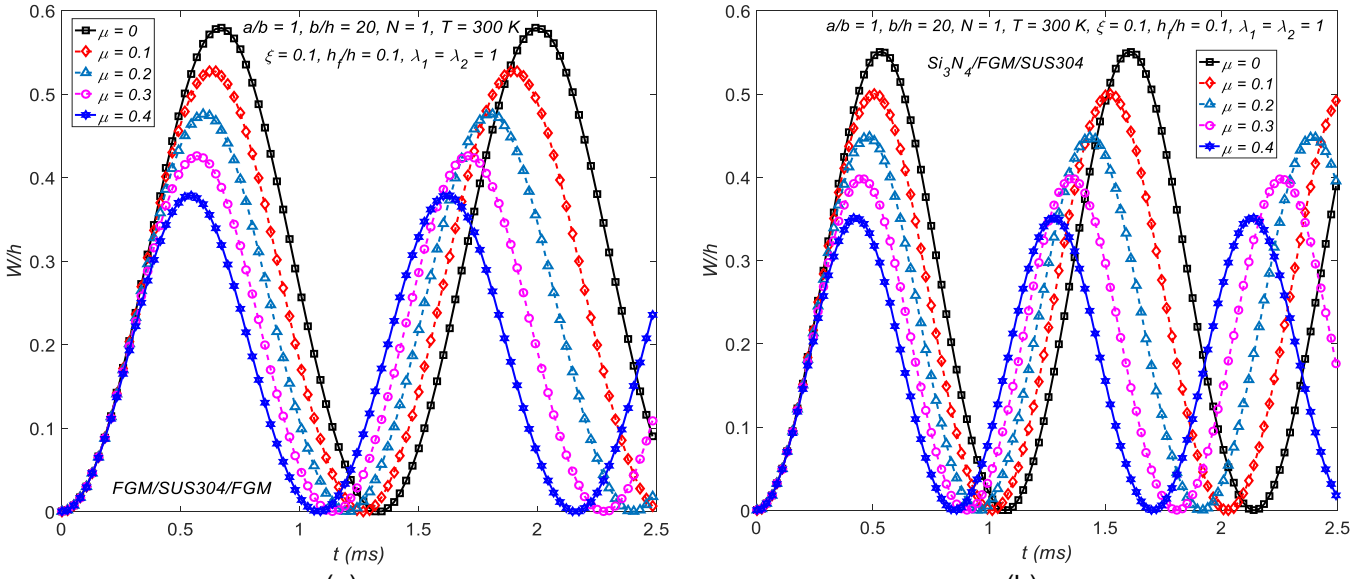

(a) (b)

Fig. 10. Effects of initial geometric imperfection on NTR of sandwich plates with immovable edges at room temperature; FGM/SUS304/FGM and (b) Si_3N_4/FGM/ SUS304

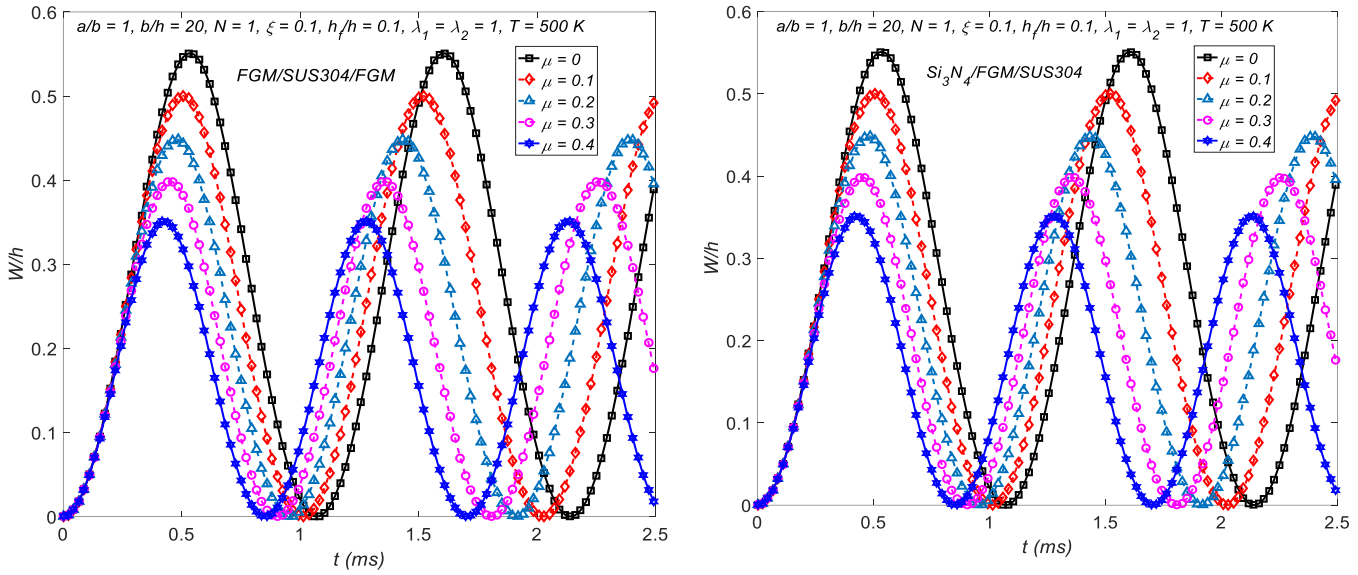

Fig. 11. Effects of initial geometric imperfection on NTR of sandwich plates with immovable edges at an elevated temperature: FGM/SUS304/FGM and (b) Si_3N_4/FGM/ SUS304

(iv) Initial geometric imperfection has considerable effects on the NTR of porous sandwich plates and the amplitude of dynamic transverse displacement is significantly decreased as the size of geometric imperfection of plate is augmented.

References

[1] G.N. Praveen, J.N. Reddy. (1998). Nonlinear transient thermoelastic analysis of functionally graded ceramic–metal plates. *International Journal of Solids and Structures*, 35(33), 4457-4476. https://doi.org/10.1016/S0020-7683(97)00253-9

[2] J.N. Reddy. (2000). Analysis of functionally graded plates. *International Journal for Numerical Methods in Engineering*, 47 (1-3), 663-684. https://doi.org/10.1002/(SICI)1097-0207(20000110/30)47:1/3%3C663::AID-NME787%3E3.0.CO;2-8

[3] J. Yang, H.-S. Shen. (2001). Dynamic response of initially stressed functionally graded rectangular thin plates. *Composite Structures*, 54(4), 497-508. https://doi.org/10.1016/S0263-8223(01)00122-2

[4] J. Yang, H.-S. Shen. (2002). Vibration characteristics and transient response of shear-deformable functionally graded plates in thermal environments. *Journal of Sound and Vibration*, 255(3), 579-602. https://doi.org/10.1006/jsvi.2001.4161

[5] X.-L. Huang, H.-S. Shen. (2004). Nonlinear vibration and dynamic response of functionally graded plates in thermal environments. *International Journal of Solids and Structures*, 41(9-10), 2403-2427. https://doi.org/10.1016/j.ijsolstr.2003.11.012

[6] X.-L. Huang, H.-S. Shen. (2006). Vibration and dynamic response of functionally graded plates with piezoelectric actuators in thermal environments. *Journal of Sound and Vibration*, 289(1-2), 25-53. https://doi.org/10.1016/j.jsv.2005.01.033

[7] A.H. Akbarzadeh, S.K. Hosseini Zad, M.R. Eslami, M. Sadighi. (2010). Mechanical behavior of functionally graded plates under static and dynamic loading. *Proceedings of the Institution of Mechanical Engineers, Part C: Journal of Mechanical Engineering Science*, 225(2), 326-333. https://doi.org/10.1243/09544062JMES2111

[8] A.M. Zenkour, M. Sobhy. (2013). Dynamic bending response of thermoelastic functionally graded plates resting on elastic foundations. *Aerospace Science and Technology*, 29(1), 7-

17. https://doi.org/10.1016/j.ast.2013.01.003

[9] H.-D. Ta, H.-C. Noh. (2015). Analytical solution for the dynamic response of functionally graded rectangular plates resting on elastic foundation using a refined plate theory. *Applied Mathematical Modelling*, 39(20), 6243-6257. https://doi.org/10.1016/j.apm.2015.01.062

[10] O. Bourihane, Y. Hilali, K. Mhada. (2020). Nonlinear dynamic response of functionally graded material plates using a high-order implicit algorithm. *ZAMM - Journal of Applied Mathematics and Mechanics*, 100(12), e202000087.https://doi.org/10.1002/zamm.202000087

[11] Y. Kiani, A.H. Akbarzadeh, Z.T. Chen, M.R. Eslami. (2012). Static and dynamic analysis of an FGM doubly curved panel resting on the Pasternak-type elastic foundation. *Composite Structures*, 94(8), 2474-2484. https://doi.org/10.1016/j.compstruct.2012.02.028

[12] Y. Kiani, M. Shakeri, M.R. Eslami. (2012). Thermoelastic free vibration and dynamic behaviour of an FGM doubly curved panel via the analytical hybrid Laplace–Fourier transformation. *Acta Mechanica*, 223, 1199-1218. https://doi.org/10.1007/s00707-012-0629-9

[13] N. Sundararajan, T. Prakash, M. Ganapathi. (2005). Nonlinear free flexural vibrations of functionally graded rectangular and skew plates under thermal environments. *Finite Elements in Analysis and Design*, 42(2), 152-168. https://doi.org/10.1016/j.finel.2005.06.001

[14] M. Talha, B.N. Singh. (2011). Large amplitude free flexural vibration analysis of shear deformable FGM plates using nonlinear finite element method. *Finite Elements in Analysis and Design*, 47(4), 394-401. https://doi.org/10.1016/j.finel.2010.11.006

[15] H.-S. Shen, Z.-X. Wang. (2012). Assessment of Voigt and Mori–Tanaka models for vibration analysis of functionally graded plates. *Composite Structures*, 94(7), 2197-2208. https://doi.org/10.1016/j.compstruct.2012.02.018

[16] A. Gupta, M. Talha. (2017). Nonlinear flexural and vibration response of geometrically imperfect gradient plates using hyperbolic higher-order shear and normal deformation theory. *Composites Part B: Engineering*, 123, 241-261. https://doi.org/10.1016/j.compositesb.2017.05.010

[17] J.-R. Cho. (2021). Nonlinear bending and free vibration analyses of metal-ceramic functionally graded plates by 2-D natural element method. *Journal of Mechanical Science and Technology*, 35(12), 5591-5599. https://doi.org/10.1007/s12206-021-1130-y

[18] F. Alijani, F. Bakhtiari-Nejad, M. Amabili. (2011). Nonlinear vibrations of FGM rectangular plates in thermal environments. *Nonlinear Dynamics*, 66, 251-270. https://doi.org/10.1007/s11071-011-0049-8

[19] V.R. Kar, S.K. Panda. (2014). Nonlinear free vibration of functionally graded doubly curved shear deformable panels using finite element method. *Journal of Vibration and Control*, 22(7), 1935-1949. https://doi.org/10.1177/1077546314545102

[20] S. Lore, A.S. Deshpande, B.N. Singh. (2024). Nonlinear free vibration analysis of functionally graded plates and shell panels using quasi-3D higher order shear deformation theory. *Mechanics of Advanced Materials and Structures*, 31(2), 453-469. https://doi.org/10.1080/15376494.2022.2114050

[21] A.M. Zenkour. (2005). A comprehensive analysis of functionally graded sandwich plates: Part 2 – Buckling and free vibration. *International Journal of Solids and Structures*, 42(18-19), 5243-5258. https://doi.org/10.1016/j.ijsolstr.2005.02.016

[22] A.M. Zenkour, M. Sobhy. (2010). Thermal buckling of various types of FGM sandwich plates. *Composite Structures*, 93(1), 93-102.

https://doi.org/10.1016/j.compstruct.2010.06.012

[23] A.M.A. Neves, A.J.M. Ferreira, E. Carrera, M. Cinefra, R.M.N. Jorge, C.M.M. Soares. (2012). Buckling analysis of sandwich plates with functionally graded skins using a new quasi-3D hyperbolic sine shear deformation theory and collocation with radial basis functions. *ZAMM - Journal of Applied Mathematics and Mechanics*, 92(9), 749-766. https://doi.org/10.1002/zamm.201100186

[24] A.M.A. Neves, A.J.M. Ferreira, E. Carrera, M. Cinefra, C.M.C. Roque, R.M.N. Jorge, C.M.M. Soares. (2013). Static, free vibration and buckling analysis of isotropic and sandwich functionally graded plates using a quasi-3D higher-order shear deformation theory and meshless technique. *Composites Part B: Engineering*, 44(1), 657-674. https://doi.org/10.1016/j.compositesb.2012.01.089

[25] N.E. Meiche, A. Tounsi, N. Ziane, I. Mechab, E.A.A. Bedia. (2011). A new hyperbolic shear deformation theory for buckling and vibration of functionally graded sandwich plate. *International Journal of Mechanical Sciences*, 53(4), 237-247. https://doi.org/10.1016/j.ijmecsci.2011.01.004

[26] A. Bessaim, M.S. Houari, A. Tounsi, S.R. Mahmoud, E.A.A. Bedia. (2013). A new higher order shear and normal deformation theory for the static and free vibration analysis of sandwich plates with functionally graded isotropic face sheets. *Journal of Sandwich Structures and Materials*, 15(6), 671-703. https://doi.org/10.1177/1099636213498888

[27] H.-S. Shen, S.-R. Li. (2008). Postbuckling of sandwich plates with FGM face sheets and temperature-dependent properties. *Composites Part B: Engineering*, 39(2), 332-344.https://doi.org/10.1016/j.compositesb.2007.01.004

[28] Z.-X. Wang, H.-S. Shen. (2011). Nonlinear analysis of sandwich plates with FGM face sheets resting on elastic foundations. *Composite Structures*, 93(10), 2521-2532. https://doi.org/10.1016/j.compstruct.2011.04.014

[29] Z.-X. Wang, H.-S. Shen. (2013). Nonlinear dynamic response of sandwich plates with FGM face sheets resting on elastic foundations in thermal environments. *Ocean Engineering*, 57, 99-110. https://doi.org/10.1016/j.oceaneng.2012.09.004

[30] H.V. Tung. (2015). Thermal and thermomechanical postbuckling of FGM sandwich plates resting on elastic foundations with tangential edge constraints and temperature dependent properties. *Composite Structures*, 131, 1028-1039. https://doi.org/10.1016/j.compstruct.2015.06.043

[31] H.V. Tung. (2017). Nonlinear thermomechanical response of pressure-loaded doubly curved functionally graded material sandwich panels in thermal environments including tangential edge constraints. *Journal of Sandwich Structures and Materials*, 20(8), 974-1008. https://doi.org/10.1177/1099636216684312

[32] D.T. Dong, V.H. Nam, N.T. Trung, N.T. Phuong, V.T. Hung. (2020). Nonlinear thermomechanical buckling of sandwich FGM oblique stiffened plates with nonlinear effect of elastic foundation. *Journal of Thermoplastic Composite Materials*, 35(10), 1441-1467. https://doi.org/10.1177/0892705720935957

[33] V.H. Nam, N.T. Phuong, N.T. Trung. (2019). Nonlinear buckling and postbuckling of sandwich FGM cylindrical shells reinforced by spiral stiffeners under torsion loads in thermal environments. *Acta Mechanica*, 230, 3183-3204. https://doi.org/10.1007/s00707-019-02452-5

[34] N. Wattanasakulpong, V. Ungbhakorn. (2014). Linear and nonlinear vibration analysis of elastically restrained ends FGM beams with

porosities. *Aerospace Science and Technology*, 32(1), 111-120. https://doi.org/10.1016/j.ast.2013.12.002

[35] N.D. Anh, N.V. Thinh, H.V. Tung. (2024). Nonlinear vibration analysis of geometrically imperfect FGM Timoshenko beams with porosity and elastically restrained ends in thermal environments. *Mechanics Based Design of Structures and Machines*, 52(12), 10148-10169. https://doi.org/10.1080/15397734.2024.2353876

[36] A.S. Rezaei, A.R. Saidi, M. Abrishamdari, M.H. Pour Mohammadi. (2017). Natural frequencies of functionally graded plates with porosities via a simple four variable plate theory: an analytical approach. *Thin-Walled Structures*, 120, 366-377. https://doi.org/10.1016/j.tws.2017.08.003

[37] N.V. Thinh, H.V. Tung. (2024). Free vibration and dynamical analyses of FGM plates with porosity and tangential edge constraints. *Journal of Vibration Engineering & Technologies*, 12, 5291-5305. https://doi.org/10.1007/s42417-023-01205-y

[38] X. Hu, T. Fu. (2023). Free vibration analysis of functionally graded plates with different porosity distributions and grading patterns. *Journal of Mechanical Science and Technology*, 37, 5725-5738. https://doi.org/10.1007/s12206-023-1012-6

[39] S. Zghal, F. Dammak. (2021). Vibration characteristics of plates and shells with functionally graded pores imperfections using an enhanced finite shell element. *Computers and Mathematics with Applications*, 99, 52-72. https://doi.org/10.1016/j.camwa.2021.08.001

[40] L.T.N. Trang, N.V. Thinh, H.V. Tung. (2024). Vibration and thermomechanical transient response of doubly curved FGM panels with porosities and elastically restrained edges. *Mechanics Based Design of Structures and Machines*, 52(8), 4907-4929. https://doi.org/10.1080/15397734.2023.2242486

[41] B.W. Abuteir, D. Boutagouga. (2022). Free-vibration response of functionally graded porous shell structures in thermal environments with temperature-dependent material properties. *Acta Mechanica*, 233, 4877-4901. https://doi.org/10.1007/s00707-022-03351-y

[42] K. Xie, Y. Wang, H. Niu, H. Chen. (2020). Large-amplitude nonlinear free vibrations of functionally graded plates with porous imperfection: A novel approach based on energy balance method. *Composite Structures*, 246, 112367. https://doi.org/10.1016/j.compstruct.2020.112367

[43] P.M. Ramteke, V. Kumar, N. Sharma, S.K. Panda. (2022). Geometrical nonlinear numerical frequency prediction of porous functionally graded shell panel under thermal environment. *International Journal of Non-Linear Mechanics*, 143, 104041. https://doi.org/10.1016/j.ijnonlinmec.2022.104041

[44] P.M. Ramteke, S.K. Panda, N. Sharma. (2022). Nonlinear vibration analysis of multidirectional porous functionally graded panel under thermal environment. *AIAA Journal*, 60(8), 4923-4933. https://doi.org/10.2514/1.J061635

[45] N.D. Anh, N.V. Thinh, H.V. Tung. (2024). Nonlinear thermomechanical vibration of initially stressed functionally graded plates with porosities. *ZAMM - Journal of Applied Mathematics and Mechanics*, 104(2), e202300528. https://doi.org/10.1002/zamm.202300528

[46] N.V. Thinh, H.V. Tung. (2025). Nonlinear thermal vibration and postbuckling of shear deformable porous FGM circular plates with geometric imperfection and elastic edge restraint. *Mechanics Based Design of Structures and Machines*, 53(10), 6765-6788. https://doi.org/10.1080/15397734.2025.2489068

[47] L.T.N. Trang, V.T. Long, N.V. Thinh, H.V. Tung.

(2025). Mechanical and thermal nonlinear buckling analysis of FGM shallow spherical caps with porosity and elastically restrained edge. *ZAMM - Journal of Applied Mathematics and Mechanics*, 105(10), e70264. https://doi.org/10.1002/zamm.70264

[48] H.V. Tung, N.V. Thinh. (2025). Thermomechanical nonlinear vibration of axially loaded functionally graded material cylindrical panels including porosity. *AIAA Journal*, 63(3), 1091-1105. https://doi.org/10.2514/1.J064613

[49] H.V. Tung, N.V. Thinh. (2025). Nonlinear free vibration of geometrically imperfect porous FGM shell panels on nonlinear foundations including elastic edge restraints and elevated temperatures. *Acta Mechanica*, 236, 1091-1115. https://doi.org/10.1007/s00707-024-04207-3

[50] Z. Lakhdar, S.M. Chorfi, S.A. Belalia, K.M. Khedher, A.E. Alluqmani, A. Tounsi, M. Yaylaci. (2024). Free vibration and bending analysis of porous bi-directional FGM sandwich shell using a TSDT p-version finite element method. *Acta Mechanica*, 235, 3657-3686. https://doi.org/10.1007/s00707-024-03909-y

[51] J.N. Reddy. (2004). Mechanics of laminated composite plates and shells: theory and analysis. *CRC Press*.

[52] L. Librescu, W. Lin. (1997). Vibration of thermomechanically loaded flat and curved panels taking into account geometric imperfections and tangential edge restraints. *International Journal of Solids and Structures*, 34(17), 2161-2181. https://doi.org/10.1016/S0020-7683(96)00025-X